Hollow waveguide for urology treatment

H. Jelínková[a*], M. Němec[a], P. Koranda[a], J. Pokorný[b], O. Kőhler[b], P. Drlík[b], M. Miyagi[c], K. Iwai[c], Y. Matsuura[d]

[a]*Czech Technical University in Prague, Faculty of Nuclear Sciences and Physical Engineering, Břehová 7, 115 19 Prague 1, Czech Republic*
e-mail:hjelin@troja.fjfi.cvut.cz
[b]*Central Military Hospital, Clinic of Urology, U vojenské nemocnice 2 169 02 Prague 6, Czech Republic*
[c]*Sendai National College of Technology 4-16-1 Ayashi Chuo, Aoba-ku, Sendai, Japan*
[d]*Tohoku University, Graduate School of Engineering, Department of Electrical Communications, Sendai 980-8579, Japan*

Abstract The aim of our work was the application of a special sealed hollow waveguide system for urology treatment. In our experimental study we have compared the effects of CTH:YAG (wavelength 2100 nm) and Er:YAG (wavelength 2940 nm) laser radiation both on human urinary stones (or compressed plaster samples which serve as a reference) fragmentation and soft ureter tissue incision in vitro. Cyclic Olefin Polymer – coated silver (COP/Ag) hollow glass waveguides with inner and outer diameters 700 and 850 μm, respectively, were used. To prevent any liquid to diminish and stop the transmission, the waveguide termination was utilized.

Keywords: hollow waveguide, urology, ureter, lithotripsy, solid state laser, Er:YAG laser, CTH:YAG laser

1. INTRODUCTION

While optical fibers are utilized as standard delivery systems in visible and near-infrared ranges of radiation, the transfer of radiation in mid-infrared radiation region or the powerful radiation requires a special delivery system, i.e., an articulated arm, special fiber, or o waveguide. The selected hollow waveguides have several advantages. Due to air core they have a high power damage threshold, low insertion losses, and no end reflection. At present the effort to obtain a more effective and fragile delivery system results in developing new waveguide types useful for the application of laser radiation in new industrial technology systems or in medicine.
This work is a continuation of our long-time investigation of laser radiation delivery in a broad region of wavelengths (from
750 nm to 2940 nm) by hollow waveguides with the inner diameter ranging from 250 μm to 1 mm in which the laser systems worked in free-running, Q-switching, or mode-locking regimes. The energy, temporal, and spatial characteristics were studied. Also, application in some treatment was demonstrated. The goal of this work was to describe the delivery system for Er:YAG laser and its use in urology.

2. MATERIALS AND METHODS

Over the past twenty years a variety of laser systems has been tested for urology surgery such as: treatment of urethral and ureteral strictures, treatment of BPH (benign prostatic hyperplasy), or stone disintegration (lithotripsy). So far, the long-term results of the stricture treatment are not fully sufficient, due to a high rate of recurrence. Therefore, new methods of treatment in which the ureter tissue vicinity will not be affected are highly appreciated.
If laser radiation is used for this treatment, the ureter tissue must be ablated. The depth of the vaporized channel mainly depends on spectral absorption of the radiation in a tissue, and, as water is a prominent component of biological tissues, this depth is mainly given by the absorption of laser radiation in water. In the mid-infrared region, a family of solid state lasers (based on Er, Tm or Ho ions) is available whose radiation has sufficient absorption in OH-containing media [1]. From literature is known promising obtained results with Er:YAG laser radiation applied during animal treatment [2].
The objective of this study was to investigate and compare the ablation effect of selected mid-infrared laser radiations (Tm:YAG, CTH:YAG, CTE:YAG, and Er:YAG) on human ureter tissue, an verification of perforation possibility of the

Optical Fibers and Sensors for Medical Diagnostics and Treatment Applications X, edited by Israel Gannot, Proc. of SPIE Vol. 7559, 755907 · © 2010 SPIE · CCC code: 1605-7422/10/$18 · doi: 10.1117/12.840916

ureter wall by these types of lasers; and investigation of basic interaction characteristic with its surface and deep structure.

2. EXPERIMENTAL METHODS

2.1 Radiation delivery system

For laboratory laser systems, the radiation delivery system consists of three parts - a coupling lens, waveguide, and cap. The coupling lens was selected according to the focusing beam spot diameter and inner waveguide diameter. In our case, a CaF_2 lens with focal length 40 mm was utilized.

The main part of the delivery system was a polymer-coated silver hollow glass waveguides suitable to deliver high-power mid-infrared Er:YAG radiation. The detailed structure of this waveguide type is the following – its basis is a fused silica capillary with the inner diameter 100-1000 μm and length up to 2 m. On the inner surface of this tube there is a silver thin film with a dielectric layer of cyclic olefin polymer (COP). The layer from this material increases the reflectance of delivered radiation. The thickness of the dielectric layer depends on the radiation wavelength and for 2.94 μm it was 0.1 μm.

The advantages of COP/Ag hollow glass waveguides are low-loss property, low aging effect, and, moreover, they are non-toxicity. Due to the absence of a bulk material in which the radiation is transmitted, hollow waveguides have usually lower losses, and, in contrast to the known silica fibers, special low-OH silica, or germanium fibers, they can also deliver high power radiation.

The utilized samples of the 10 cm long waveguide were 700 μm in the inner diameter and 850 μm in the outer diameter.

The frequent requirement for medical applications is that the end of the waveguide system is to be in contact with the interacting soft or hard tissue, the so-called "contact treatment"; therefore the hollow waveguide end was terminated with a special sealed waveguide cap (Fig.1b). This termination was first used to prevent damage to the delivery system caused by the debris and liquids entering the unsealed waveguide. This termination cap also served for radiation focusing[6]. For our experiment, fused silica was used as cap material.

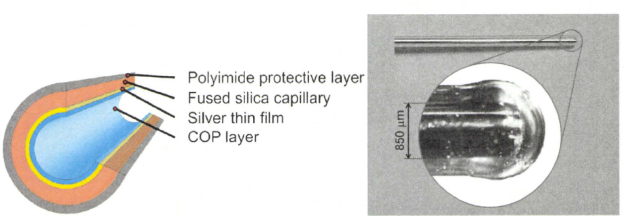

Figure 1. Layer structure of the COP/Ag hollow glass waveguide used for mid-infrared laser radiation delivery (left), detailed photo of waveguide termination (right).

2.2 Laser systems

During the experimental investigation, different laser systems were utilized, namely clinical CTH:YAG laser (Coherent Versa Pulse Power Suite Holmium), laboratory CTH:YAG (Cr,Tm,Ho:YAG) laser, and laboratory Er:YAG laser. Their basic characteristics are summarized in Table 1.

Table 1. Laser systems parameters

	Clinical CTH:YAG	Laboratory CTH:YAG	Laboratory Er:YAG
Wavelength	2100 nm	2100 nm	2940 nm
Rep. rate	5-25 Hz	1 Hz	1 Hz
Max. energy	20 J	300 mJ	300 mJ

2.2.1 Er:YAG laser system

In Er:YAG laser oscillator (λ = 2.94 μm), an active crystal 5 mm in diameter and 100 mm long was used along with xenon flashlamp. These elements were placed inside a diffused ceramic pumping cavity. The resonator consists of plane total reflecting copper mirror and an output coupler with the optimal reflectivity R_{out} = 80 %. The generated wavelength was 2.94 μm, and the pulse duration was measured to be 190 μs (FWHM). The radiation was delivered to the target tissue by a special hollow waveguide, (see section 2.1) so the fluence on tissue reached 78 J/cm^2.

2.2.2 CTH:YAG laser system

The laser head of CTH:YAG laser (λ = 2.1 μm) consists of a Cr:Tm:Ho:YAG crystal with a diameter of 4 mm and a length of 89 mm placed, along with a xenon flashlamp into a diffused ceramic pumping cavity (Marysol Technologies, Inc.). The resonator had plane-parallel configuration and was formed by two mirrors with the reflectivity R = 100% and R_{out} = 83 %. The interaction experiment we have started with the same energy being measured behind the hollow waveguide delivery system 100 mJ (fluence 26 J/cm^2). Because the perforation was not obtained, higher energy up to 400 mJ (which corresponds to a fluence of 104 J/cm^2) was applied.

2.2.3. Clinical CTH:YAG laser

The clinical CTH:YAG laser (Coherent Versa Pulse Power Suite Holmium) was a flashlamp-pumped CTH:YAG laser with higher repetition rate (from 5 up to 25 Hz). The maximal output power was 100 W. Its radiation was delivered by a low-OH fibre with the diameter 400 μm.

2.3 Examined Sample Preparation

For the purpose of soft tissue experiment, the samples in the form of longitudinal sections (approximately 4x30 mm) 1 to 1.5 mm thick (Figure 2) were used. They were stored in a refrigerated saline solution and the experiments were performed in vitro within three hours after the surgery at room-temperature.

For the purpose of lithotripsy, experiments on both artificial and real human samples were performed. In case of artificial samples, the blocks made from special compressed plaster (size 10x10 mm, thickness from 1 up to 10 mm, producer Stolz, Inc.) were utilized (Figure 3). As to real human samples, the urinary stones (size approximately 7x5x3 mm) of various composition were utilized (Figure 4).

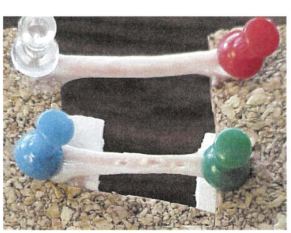

Figure 2: Human ureter tissue sample.

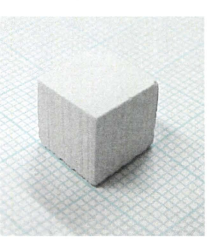

Figure 3: Artificial sample made from compressed plaster serving as urinary stone model.

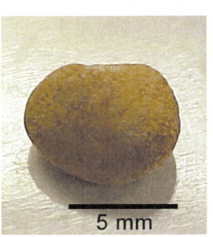

Figure 4: Human urinary stone.

2.4 Measuring instruments

To investigate the output laser radiation energy, we used a computer-operated two channel Molectron JD2000 Joulemeter/Ratiometer and Tektronix TDS 3052B oscilloscope with thermal detectors Gen-Tec (ED-200 LA) and Molectron (J25). During the interaction process, ablated holes were investigated by a microscope (Nikon SMZ-2T).

2.5 Experimental Methods

The ureter sample was mounted in a special holder directly attached to a movable stage. The end of sealed waveguide was in contact with the tissue. The specimens of the ureter tissues were gradually irradiated by the CTH:YAG, and Er:YAG radiations. The laser radiation was delivered to the interaction sample by a COP/Ag hollow glass waveguide (inner/outer diameter 700/850 um, length 10 cm) terminated with a fused silica cap. The interaction experiments were carried out in contact regime.

The input waveguide energy was monitored with a beam splitter placed in front of the waveguide input and the first Joulemeter head. At the same time, the output energy was monitored with the second energy detector placed behind the hollow waveguide termination. After the measurement of the output energy, the investigated tissue sample was inserted between the waveguide termination and the probe. The first coming impulse was monitored on the scope when tissue was perforated.

2.6 Analysing Methods

After laser ablation, the samples of tissue were photographed and pickled in formaldehyde. Then, the soft specimens were taken for H&E staining and histological processing.

3. EXPERIMENTAL RESULTS

3.1 Perforation of soft ureter tissue with laser radiation

For soft ureter tissue, the primary desired result is perforation or incision of the tissue. The aim was to determine the optimal laser wavelength, pulse energy, and length from the point of operation effectiveness and minimization of the adjacent tissue alteration. The interaction parameters are summarized in the following table:

Table 2: Laser interaction parameters for ureter tissue perforation

Laser	Pulse energy	Pulse duration	Energy fluence	Radiation intensity	Ablation threshold	Ablation rate	Mesenchyme alteration
	mJ	μs, ns	J/cm^2	W/cm^2	J/cm^2	mm/pulse	μm
CTH:YAG	200	200 μs	54	260x10^3	20	0.008	200
Er:YAG Free-running	100	200 μs	27	130x10^3	6	0.05	50
Er:YAG Q-switching	30	60 ns	8	111x10^6	2	0.2	Not visible

Examples of the compared laser radiations interactions with soft ureter tissue are shown in the following pictures.

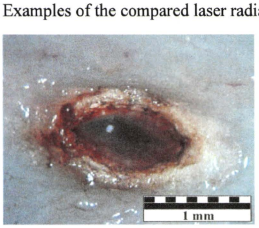

Figure 5 CTH:YAG laser: 100 pulses with energy 200 mJ and duration 200 μs – macrophotography.

Figure 6 Er:YAG free-running: 20 pulses with energy 100 mJ and duration 200 μs – macrophotography.

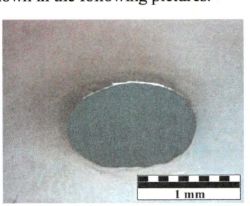

Figure 7 Er:YAG Q-switching: 5 pulses with energy 30 mJ and duration 60 ns – macrophotography.

All the relevant ureter samples were histologically examined from the point of view of adjacent tissue thermal damage.

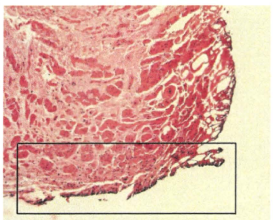

Figure 8 CTH:YAG laser: 100 pulses with energy 200 mJ – histological evaluation.

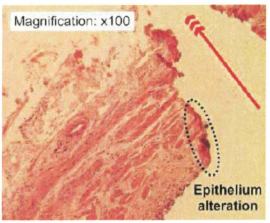

Figure 9 Er:YAG free-running: 20 pulses with energy 100 mJ and duration 200 μs – histological evaluation.

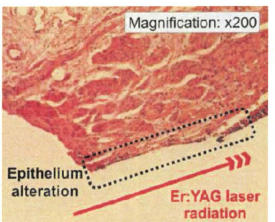

Figure 10 Er:YAG Q-switching: 5 pulses with energy 30 mJ and duration 60 ns – histological evaluation.

3.2 Fragmentation of urinary stones by laser radiation

The desired result in laser-assisted lithotripsy is the minimally invasive fragmentation of urinary stones. The aim of our study was to compare the effectiveness of laser radiation interaction with urinary stones or artificial samples model. During the interaction experiments the samples were stored in water at room-temperature. As for laboratory lasers, the radiation was delivered to the interaction samples with the help of COP/Ag hollow waveguide terminated with a fused silica cap. The cap was in water and in contact with samples. In case of clinical CTH:YAG laser, the radiation was delivered by the fibre.

We have evaluated the ablation effect for various laser pulse energies and various number of pulses. From the obtained experimental data we have analyzed the perforation rates for both investigated laser radiations. The laser repetition rate was 1 Hz (in the case of laboratory lasers) and 20 Hz (in the case of clinical CTH:YAG laser). Upon the experiments, it has been determined how many laser pulses (with defined pulse energy) are required for sample perforation. The results are summarized in the following Figures 11-13.

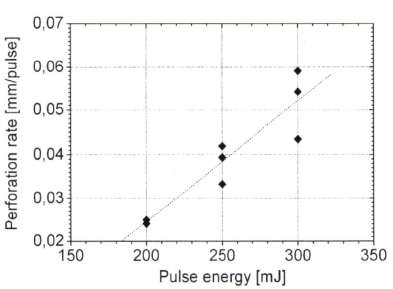

Figure 11. Perforation rate of artificial stones (compressed plaster) ablated with Er:YAG laser radiation.

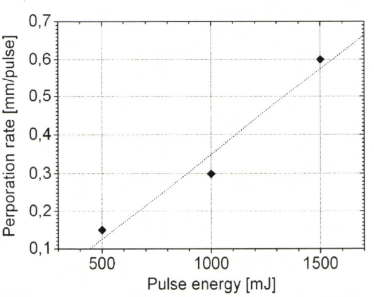

Figure 12. Perforation rate of artificial stones (compressed plaster) ablated with CTH:YAG laser radiation.

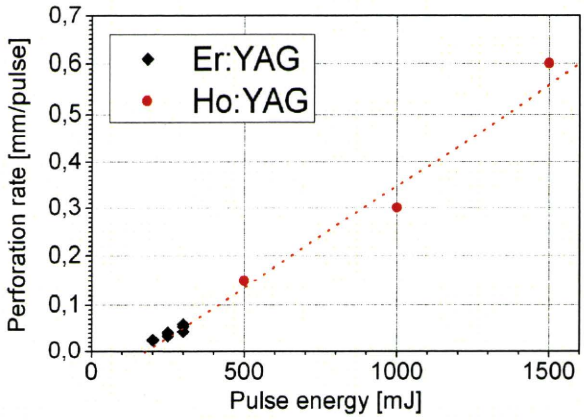

Figure 13. Comparison of perforation rates of artificial stones (compressed plaster) ablated with Er:YAG or CTH:YAG laser radiation.

4. DISSCUSSION

From the experimental results it could be evaluated that Er:YAG laser radiation (2940 nm) is more effective in ablation of soft ureter tissueas against the CTH:YAG laser. The reason could be in the absorption coefficient of radiation in water (soft ureter tissue has high content of water), which is wavelength-selective (especially in the mid-infrared region) and the Er:YAG laser radiation matches the local maximum of this absorption spectrum (Figure 14). Even more effective is the Er:YAG laser in Q-switched operation regime, where the pulse duration is approximatelly three orders of magnitude shorter than in the free-running regime. Therefore, the thermal damage to adjacent tissue is significantly lower.

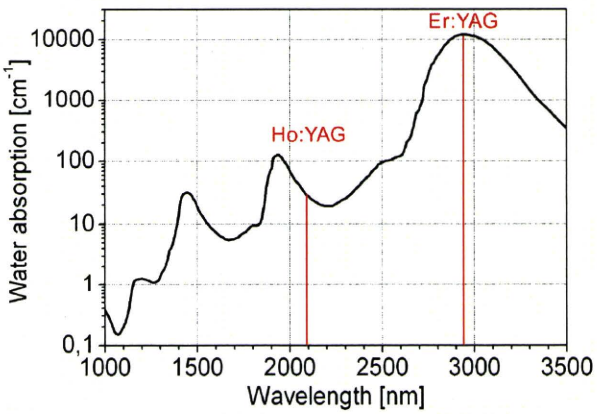

Figure 14: Spectral characteristics of water absorption in mid-infrared region.

Pulse energies which can perforate the ureter wall were found for CTH:YAG, and Er:YAG laser radiation. The Er:YAG laser radiations demonstrate minor surface carbonization in comparison with CTH:YAG radiation. Applications of those radiations led to quite minimum deep structures alteration, not exceeding 0.2 mm.

In case of laser-assisted lithotripsy, the effect of the Er:YAG laser radiation is comparable with the CTH:YAG laser radation. The difference is in the energy level required for the application. In case of Er:YAG laser, the pulse energy needed for urinary stone ablation is lower.

5. CONCLUSION

Our conclusion is that both CTH:YAG, and Er:YAG lasers can be used for wall ureter perforation. However differences were observed in the quality of the ablated surface. From the histology point of view, the great differences have been seen in tissue modifications of both - the epithelium and mesenchym. Thus, from our study it follows that the Er:YAG lasers could be considered as good candidates for urology surgery. The delivery system formed by Cyclic Olefin Polymer – coated silver (COP/Ag) hollow glass waveguide was found to be a good instrument for delivery of mid-infrared radiation and also reliable component for urology surgery.

6. ACKNOWLEDGEMENTS

This research has been supported by the Grant of the Czech Ministry of Education No.MSM6840770022 "Laser systems, radiation and modern optical applications" as well as by the Monbusho Grant-in-aid for Scientific Research (B)(2), No.11694120 of Japan.

7. REFERENCES

[1] Boulnois J. L., "Photophysical processes in recent medical laser developments: A review", Lasers in Medical Science, 47-66 (1986)

[2] Fried, N.M. and Long, G.M., "Erbium:YAG laser ablation of urethral and ureteral tissues", Proc. SPIE 4609, 122-127 (2002).

[3] Shi, Y.W., Hanamoto, K., Wang, Y., Abe, Y., Matsuura, Y., Sato, S. and Miyagi, M., "New cyclic olefin polymer-coated silver hollow glass waveguides for the near-infrared to mid-infrared", Proc. SPIE 3570, 4-11 (1998).

[4] Jelínková H., Miyagi M., Šulc J., Černý P., Shi Y., Matsuura Y. and Takada G., "Delivery of Powerful Radiation in Visible Spectral Region by Special Waveguides", Proc. SPIE 4253, 58-67 (2001).

[5] Jelinkova, H., Nemec, M., Sulc, J., Miyagi, M., Iwai, K., Abe, Y., Shi, Y.W., Matsuura, Y. and Pasta, J., "Transmission Characteristics of Sealed Hollow Waveguides for Er:YAG Laser Radiation and Their Application in the Ophthalmology", Proc. SPIE 4616, 135-142 (2002).

[6] Iwai, K., Shi, Y.-W., Endo, M., Ito, K., Matsuura, Y., Miyagi, M. and Jelinkova, H., "Penetration of high-intensity Er:YAG laser light emitted by IR hollow optical fibers with sealing caps in water", Applied Optics 43, No. 12, 2568-2571 (2004).

FT-IR based loss-spectrum measuring-system for infrared hollow waveguides

Cong-Hui Yang [1], Hua Hua [1], Wei Tan [1], Yi-Wei Shi [1]*, Katsumasa Iwai [2], and Mitsunobu Miyagi [2]

1) Department of Communication Science and Engineering, Fudan University, Handan Rd. 220, Shanghai 200433, China.
2) Sendai National College of Technology, Sendai, 989-3128, Japan
* Email: ywshi@fudan.edu.cn

ABSTRACT:

A loss-spectrum measuring-system for hollow waveguides was established based on the Fourier Transform infrared Spectrometer (FTIR). In order to obtain better repeatability, we designed and fabricated two couplers for the system. One is a silver-coated hollow tube with the same inner diameter as the measured hollow waveguide. The other is a silver-coated tapered coupler whose inner diameter of the output end is the same as the measured hollow waveguide. Characteristics of the measuring system were discussed theoretically and experimentally when using the two couplers. Several kinds of hollow waveguides were measured and the properties of the loss spectra were discussed. The measured loss property showed that loss property depends on the output divergence angle of the coupler. Tapered coupler has a much larger output divergence than that of the hollow tube. Both of the couplers attains stable coupling with the hollow waveguides. Loss spectra were successfully measured for hollow waveguides with the length ranging from several centimeters to 3 meters.

Keywords: hollow waveguides, FTIR, tapered coupler, measuring system, loss spectrum, divergence angle

1. INTRODUCTION

A hollow-core waveguide has the advantages of relatively simple structure and low cost. Especially in the mid-infrared region, a hollow-core waveguide has advantages over a solid-core waveguide, such as low loss and high laser-induced-damage threshold[1-3]. There are two types of hollow-core waveguides: those with wall materials that has a refractive index n less than one (ATR guides) and waveguides whose wall materials has a refractive index n greater than one (Leaky guides) [2-3]. ATR guides may include the GeO_2 coated hollow waveguides and hollow sapphire waveguides. GeO_2 waveguides are fabricated by depositing GeO_2 film inside glass tubing. Hollow sapphire waveguides are single crystal waveguides growth by the laser heated pedestal growth (LHPG) method. The dielectric/metal coated hollow waveguides, whose wall materials refractive index n is greater than one, are leaky guides. They are fabricated by depositing metallic and dielectric coating inside capillary tubing. Loss spectra of the waveguides show the properties of film material absorptions and interference peaks and valleys. The information is useful to optimize the waveguide fabrication such as dielectric material choice and the thickness of the inner-coating films. By using the low-loss waveguides as a sensing head, absorption and reflectance properties and transmittance for different materials or gases

Optical Fibers and Sensors for Medical Diagnostics and Treatment Applications X, edited by Israel Gannot, Proc. of SPIE Vol. 7559, 75590R · © 2010 SPIE · CCC code: 1605-7422/10/$18 · doi: 10.1117/12.841916

can be obtained. The positions and strength of the absorption peaks are related with the materials ingredients and their concentration. Applications in gas sensing and endoscope measurements are applications that are based on the low-loss properties both in the mid-infrared and the far-infrared of the hollow waveguides.

We propose the use of Fourier Transform infrared Spectrometer (FTIR) to establish the loss-spectrum measuring-system in the mid-infrared region. The dielectric/metal coated hollow waveguides, GeO_2 coated hollow waveguides and hollow sapphire waveguides were measured by using the system. Repeatability was obtained for the loss spectrum. Theoretical calculations were also conducted for the abovementioned waveguides according to the loss theory of circular hollow waveguides.

2. MEASURING SYSTEM

Figure 1 shows the optical path of a FTIR. With the reflector in the middle, light is guided out of FTIR device and coupled into the measuring waveguide. The output energy of the waveguide sample was measured by the external detector. The optical reflections shown in dashed lines were the original optical transmission before FTIR modification. We build the sample compartment on the external optical platform. Together with the external detector, the loss-spectrum measuring-system is established. It can measure waveguides with a length from several centimeters to several meters.

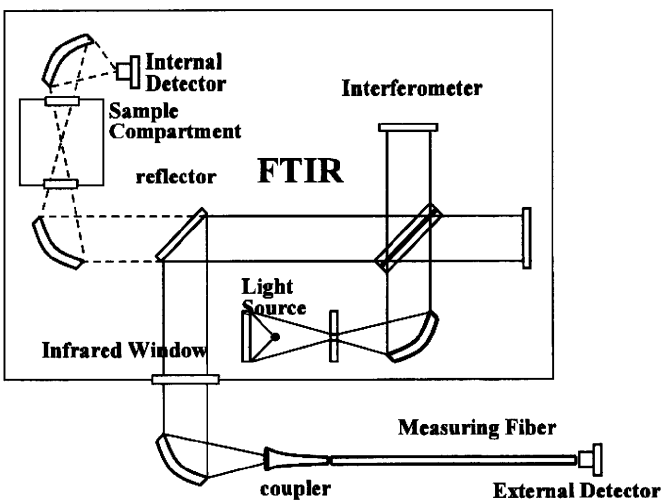

Fig.1 Schematic setup for the measuring system before and after optical path modification

The coupler in Figure 1 is one of the most important components and has a great influence on the coupling efficiency of light source to the measuring waveguide. The transmission modes, signal-to-noise ratio (SNR) and attenuations of the measured results may also be affected. Therefore, we designed and fabricated two kinds of couplers for the system. One is a silver-coated hollow waveguide coupler. The other is a silver-coated hollow tapered coupler. Inner diameter at the output end is the same as the measured hollow waveguide for both couplers. This helps to achieve the stability of coupling efficiency. Figure 2 are images of the coupling system and the two couplers. In figure 2(a), light is reflected into the coupler by a focused reflector and coupled into the waveguide through the coupler. In figure 2(b), two couplers are the same in length. The tapered coupler is better in light-gathering because of its big-bore at the input end. This

results a good coupling efficiency and better SNR in the measuring results. However, tapered coupler has a larger divergence angle at the output. It excites more higher-order modes with high propagation losses in the waveguide.

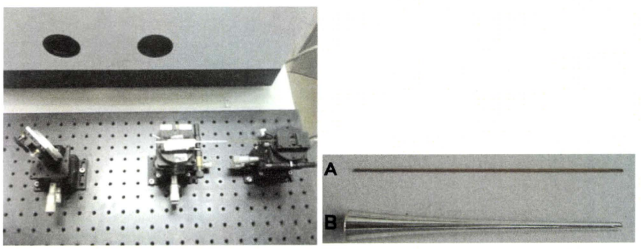

(a) (b)

Fig.2 Pictures of the coupling system (a) and the couplers (b). A is the waveguide coupler. B is the tapered coupler.

We first selected two dielectric-coated silver hollow waveguides, the dielectric materials were silver iodide and OC300, respectively. Figure 3(a) shows the loss spectrum of AgI/Ag coated hollow waveguide [3]. The length of this waveguide is 1107 mm and the inner-diameter is 0.7 mm. No obvious absorption for the AgI film can bee seen in the mid-infrared region. The peak at 2 μm is caused by the interference of light in the AgI film. Peaks at 4.3 μm and around 6 μm are caused by the absorption of CO_2 gas and water vapor in the air. Figure 3(b) is the loss spectrum of OC300/Ag coated hollow waveguide[4]. The length of the waveguide is 785 mm and the inner-diameter is 0.7 mm. Peaks at the wavelength band of 3.5 μm and 8-13 μm are caused by the intrinsic absorption of the OC300 film.

Loss spectra were measured with both couplers for the two waveguides, as shown in figure 3. Waveguides were measured several times in a few days. Loss spectrum for each waveguide was confirmed with good repeatability. We note that spectra obtained by using different couplers were almost the same, only differ in the absolute attenuation value.

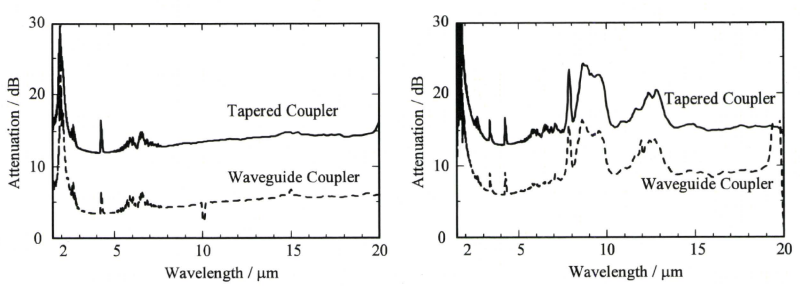

(a) (b)

Fig.3 Measured loss spectra of leaky infrared hollow waveguides using different light source coupler

3. DISCUSSIONS AND RESULTS

As shown in figure 3, measured loss spectra were different when using different couplers for the same waveguide. The tapered coupler caused a higher loss than the waveguide coupler. Analysis indicates that the attenuation of hollow waveguides is related to the divergence angle of light source. A larger angle will excite more higher-order modes, which have higher loss. In the measuring system, the light has larger divergence angle after the transmission through the tapered coupler than the waveguide coupler[5]. Therefore, the spectrum measured by using tapered coupler has higher loss.

We measured the divergence angles at the output end of both couplers. Take two normal planes at the output end of the coupler and scan the light intensity. Figure 4 plots the intensity distribution. Both planes are over 3 mm away from the output end and z1 is closer. According to the intensity distribution, we calculated full width of half maximum (FWHM) of each plane. The divergence angle of the light can be obtained by using the FWHMs and the distance between the normal planes. It is 5.7 degrees along X-axis and 11.5degrees along Y-axis. The light intensity showed the Gaussian distribution. For tapered coupler, the result is 16 and 98 degrees, respectively. The light intensity distribution is shown in figure 5. As lots of high-order modes exist, the distribution deviates from the Gaussian distribution and has several peaks. Also, distributions of both couplers are elliptical because of the properties of the light source and the light-guiding system in FTIR.

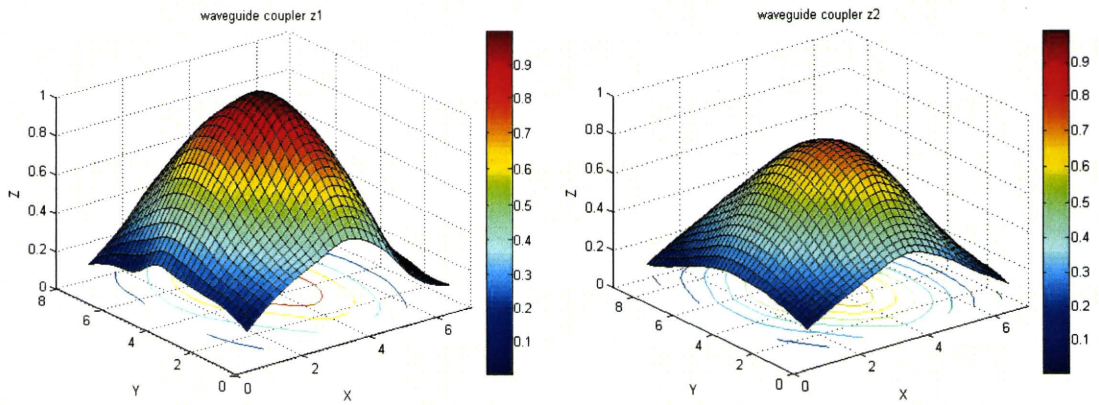

Fig.4 Profile of light intensity distribution at the output end of the waveguide coupler: Z1 (left) and Z2 (right)

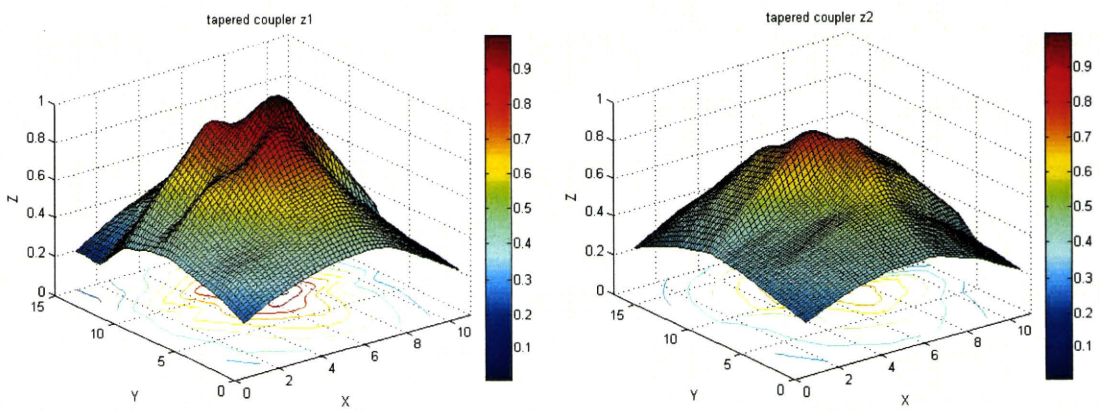

Fig.5 Profile of light intensity distribution at the output end of the tapered coupler: Z1 (left) and Z2 (right)

The transmitted power $P(z)$ in hollow waveguides is expressed as[6]

$$P(z)=\int_0^{\theta_{max}} p(\theta_z)\exp\{-[1-R(\theta_z)]z/2T\cot\theta_z\}\sin\theta_z d\theta_z$$

Where θ_{max} is the maximum launching angle, $p(\theta_z)$ is the angular distribution of the launching power, $R(\theta_z)$ is the power reflection coefficient of the light. T is the inner diameter of the waveguide. By taking the parameters of thickness, roughness of dielectric film and the divergence angle into the formula, we get the calculated result for the loss spectrum.

We took a COP/Ag coated hollow waveguide for calculation[7]. Parameters in the calculation were as follows: length, 1003 mm; inner diameter, 0.7 mm. Calculated loss spectrum is shown in figure 6 as well as the measured result. The measured spectra using different coupler are shown in fig 6 (a) for the waveguide coupler and fig 6 (b) for the tapered coupler. Peaks at 2 μm and 4 μm are caused by the interference of light in the thin COP film. Peaks at 3.5 and 7 μm are caused by the absorption of the polymer COP. In the calculation, we firstly adjust the COP film thickness to move the interference peaks to 4 μm and 2 μm. The thickness is 0.85 μm in the calculation. Then, we change the roughness of inner surface and the divergence angle of light source to make the base line of loss spectrum agree with the measured results. Roughness is 0.03 μm and the divergence angle is 15° and 45°for the waveguide coupler and tapered coupler, respectively.

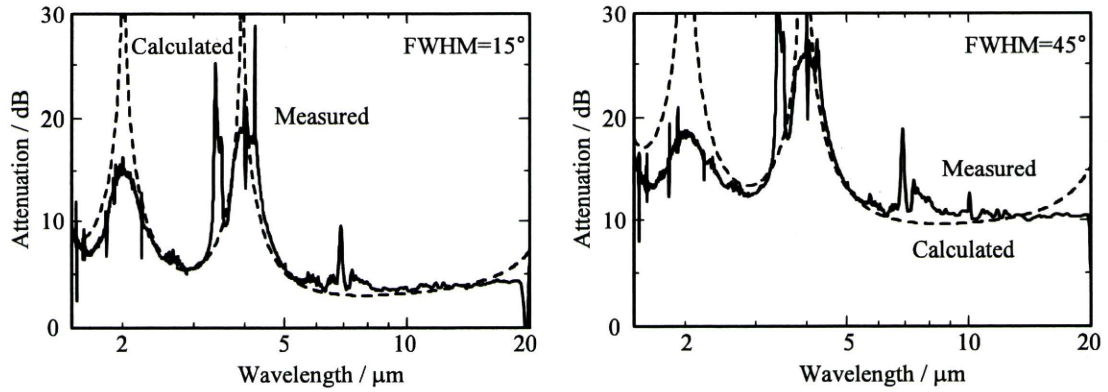

Fig.6 Calculated and measured loss spectra using different kinds of couplers

The divergence angle changes from 15 to 45 degrees in the calculation for fig 6 (a) to fig 6 (b). The other parameters are the same and the loss increases accordingly. This proves that the loss in waveguide is related with the divergence angle of light source. When the angle gets larger, the loss increases. The 3.5 and 7 μm absorption peaks disappeared in the theoretical spectrum because we did not take into consideration of the material absorption for the polymer layer in the calculation.

For ATR guides, we made the theoretical calculation for the GeO_2 coated hollow glass waveguides[8] and hollow sapphire waveguides[9]. The GeO_2 waveguide is 300 mm long and 1.4 mm in inner-diameter. Figure 7 plots the loss spectra for measured and calculated results. Low loss character can be found at 7.6 μm and within 10-12 μm. These low loss wavelength bands are caused by the properties of the materials of the base tube (SiO_2) and inner coated film (GeO_2). The refractive index n of SiO_2 around 7.6 μm is less than one, while around 10-12 μm, n of GeO_2 is less than one. According to the fabrication parameters, the GeO_2 film was of 3 μm thickness in the theoretical calculation. The surface

roughness is 0.08 μm in root mean square (rms) and the divergence angle of the light source is 20 degrees.

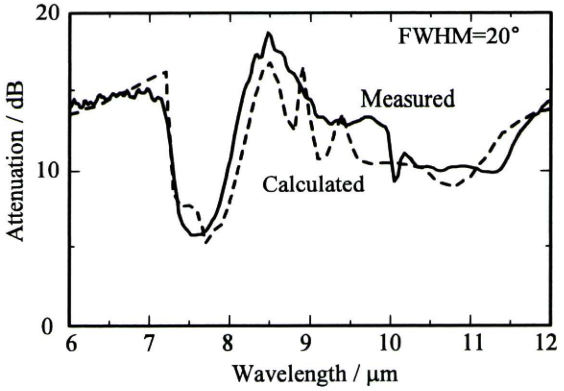

Fig.7 Calculated and measured loss spectra for GeO_2 coated hollow glass waveguide

Parameters of the selected hollow sapphire waveguide are as follows: the length is 990 mm, the inner-diameter is 1 mm. Figure 8 is the loss spectrum. The low-loss area is found from 10 to 17μm. This is because of the refractive index n of Al_2O_3 is less than one in the wavelength band. In the calculation, the divergence angle is 49 degrees.

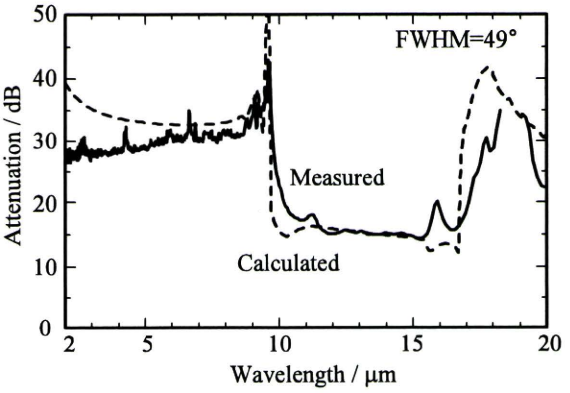

Fig.8 Calculated and measured loss spectra for hollow sapphire waveguide

From figure 7 and 8, we note that theoretical loss spectra are in accordance with the measured results both in low-loss wavelength bands and the absorption peaks. This shows that spectrum from the measuring system is reliable. Also, both the two ATR waveguides have the low loss character around 10.6 μm, which makes them both suitable for the transmission of CO_2 laser light. The refractive index of GeO_2, SiO_2 and Al_2O_3 (sapphire) used in the abovementioned calculations are from the references 10-12.

From figure 6 to 8, we used slightly different divergence angles for the same coupler. This is because the inner-diameter and roughness are not the same for these waveguides. We did not consider the influence of elliptical intensity distribution of the FTIR light source and assumed circular distribution in our calculation. The divergence angle is selected in a reasonable region. The agreement between the measured and theoretical results suggests that the measuring system is stable and reliable. The dependence of waveguide loss property on the divergence angle of the light source is also proved. Low loss property in the measured result can be attained with the waveguide coupler because of the smaller divergence angle. Better SNR result for the measurement can be obtained when using a tapered coupler.

4. CONCLUSION

In order to evaluate the film coating process and the quality of the films plated inside the infrared hollow waveguides, loss spectrum of the hollow waveguide in the mid-infrared region is normally necessary. The FTIR device usually has a compartment room of 20 cm in length, which is not capable to measuring the loss characters of a 1-3 m long infrared hollow waveguide. For the evaluation purpose, the optical path of the FTIR was modified and a sample compartment was built up on the optical platform with an external detector. The loss spectra of hollow waveguides with the length ranging from several centimeters to 3 meters were successfully measured with the new measuring system. For the stable coupling of light source into the hollow waveguides, we designed and fabricated two couplers, the waveguide coupler and the tapered coupler. The measuring system is stable and the loss spectra measured are reliable. The attenuation value differs between different couplers of the same waveguides because of the influence of the divergence angle of the light source. By the measuring results of the divergence angle and the comparison of the theoretical and measured loss spectra, the influence is confirmed. The experimental and theoretical results are helpful in the improvement of the coupling methods of the infrared spectrum measuring system and the design of the infrared waveguide sensor.

ACKNOWLEDGEMENTS

This research is supported by the National Natural Science Foundation of China (60971014), State Education Ministry (the Scientific Research Foundation for the Returned Overseas Chinese Scholars), and the 211 project for construction of key disciplines, as well as by the Ministry of Education, Sports, Science, and Technology of Japan (Basic and Fundamental Research and Development Projects B), and Health and Labor Science Research Grants (H20-nano-young-010).

REFERENCES

[1] Sui, K. R., Shi, Y. W., Tang, X. L., "Optical properties of AgI/Ag infrared hollow waveguide in the visible wavelength region" Opt. Lett. 33, 318-320 (2008).

[2] Mohebbi, M., "Transmission characteristics of femtosecond optical pulses in hollow-core waveguides" Opt. Commun. 253, 290-300 (2005).

[3] Harrington, J. A., "A review of IR transmitting, hollow waveguides" Waveguide and Integrated Optics 19, 211-227 (2000).

[4] Iwai, K., Miyagi, M., Shi, Y. W., "Infrared hollow waveguide with a vitreous film as the dielectric inner coating layer" Opt. Lett. 32, 3420-3422 (2007).

[5] Matsuura, Y., Hiraga, H., Wang, Y., "Lensed-taper launching coupler for small-bore, infrared hollow waveguides" Appl. Opt. 36, 7818-7821 (1997).

[6] Matsuura, Y., Saito, M., Miyagi, M., "Loss characteristics of circular hollow waveguides for incoherent infrared light" J. Opt. Soc. Am. A 6 (3), 423-427 (1989).

[7] Shi, Y. W., Wang, Y., Abe, Y., "Cyclic olefin polymer-coated silver hollow glass waveguides for the infrared" Appl. Opt. 37, 7758-7762 (1998).

[8] Yang, Y., Zhou, G. Y., Hou, Z. Y., "Study on Transmitting Character in GeO2 Dielectric Hollow Waveguides"

Chinese J. Lasers 31, 301-304 (2004).

[9] Gregory, C. C., Harrington, J. A., "Attenuation, modal, and polarization properties of n<1, hollow dielectric waveguides" Appl. Opt. 32, 5302-5309 (1993).

[10] Palik, E. D., [Handbook of Optical Constants of Solids vol.1], Academic Press, San Diego, 749-763 (1998).

[11] Palik, E. D., [Handbook of Optical Constants of Solids vol.3], Academic Press, San Diego, 653-682 (1998).

[12] Dobrowolski, J. A., Guo, Y., Tiwald, T., "Toward perfect antireflection coatings. 3. Experimental results obtained with the use of Reststrahlen materials" Appl. Opt. 26 (7), 1555-1562 (2006).

Loss spectrum measurement for infrared hollow fiber based on the Fourier transform infrared spectrometer

Cong-Hui Yang,[1] Hua Hua,[1] Wei Tan,[1] Katsumasa Iwai,[2] Mitsunobu Miyagi,[2] Nan Chi,[1] and Yi-Wei Shi[1,*]

[1]School of Information Science and Engineering, Fudan University, 220 Handan Road, Shanghai 200433, China

[2]Sendai National College of Technology, Sendai 989-3128, Japan

*Corresponding author: ywshi@fudan.edu.cn

Received 16 February 2010; accepted 30 March 2010; posted 7 April 2010 (Doc. ID 124332); published 26 April 2010

Based on the Fourier transform infrared spectrometer, a system for measuring the loss spectrum of hollow fiber is established. Loss spectra can be measured for hollow fibers with length ranging from several centimeters to 3 m. Two kinds of light source coupler are designed and fabricated for achieving stable coupling and a repeatable spectrum. One is a short waveguide, and the other is a tapered tube. Both are inner-coated with a silver layer and they are of the same inner diameter at the output end as the measured hollow fiber. Characteristics of the measuring system are discussed theoretically and experimentally when using the two couplers. Several kinds of hollow fibers are measured, and the properties of the loss spectra are discussed. The measured loss value is shown to be dependent on the output divergence angle of the coupler. The tapered coupler has a larger output divergence and causes higher measured loss than that of the waveguide coupler. © 2010 Optical Society of America

OCIS codes: 230.7370, 310.6860, 120.7000, 060.2270, 120.6200.

1. Introduction

Infrared hollow fiber has found applications [1–3] in medical, industrial, and sensing fields due to its advantages of simple structure, low loss, and high laser-induced-damage threshold. Hollow fibers can be grouped into two categories: those with inner wall materials that have a refractive index n of less than 1, and those with inner wall materials whose n is greater than 1. The leaky hollow fibers [4], with $n > 1$, have metallic and dielectric films deposited on the inner surface of a capillary. The attenuated total reflection (ATR) [5] hollow fibers are made of some special $n < 1$ oxide glasses. ATR hollow fibers may include GeO_2 coated [6] hollow fibers and hollow sapphire fibers [7]. GeO_2 fibers are fabricated by depositing GeO_2 film inside glass tubing. Hollow sapphire fibers are single-crystal fibers grown by the laser-heated pedestal growth method. The dielectric/metal coated hollow fibers are normally fabricated by using liquid-phase coating techniques and depositing metallic and dielectric coating inside capillary tubing.

Loss spectra of hollow fibers show the properties of film material absorptions and interference peaks and valleys. These properties in the loss spectra provide important information for optimizing the fiber fabrication, such as film material selection and the thickness of the inner coating films. By using the low-loss fiber as a sensing probe, the loss spectrum can be measured for gas absorption, reflection, and transmission properties of materials or gases. The positions and strength of the absorption peaks are related to the material ingredients and their concentration. Endoscopic measurement and laser treatment are

0003-6935/10/132504-06$15.00/0

applications that are based on the low-loss properties and high-power capability both in the mid- and far-infrared wavelength regions of the hollow fibers.

We used the Fourier transform infrared (FT-IR) spectrometer to establish a measuring system of hollow fiber for the loss spectrum in the mid-infrared (MIR) region. The dielectric/metal-coated hollow fibers, GeO_2 coated hollow fibers and hollow sapphire fibers, were measured by using the system. A repeatable spectrum was obtained for the hollow fibers. Theoretical calculations were also conducted for the above-mentioned fibers according to the loss theory of circular hollow fibers.

2. Measuring System

Figure 1 shows the optical diagram of an FT-IR. The optical reflections shown by the dashed lines were the original optical transmission before FT-IR modification. The sample compartment is about 20 cm long. It is difficult to measure a sample longer than the compartment. To measure the loss property of infrared hollow fiber, the beam was guided out of the FT-IR spectrometer through the infrared window by the reflector at the center. The beam was focused by an elliptical mirror and coupled into a coupler. The output energy of the coupler and measured fiber were measured by the external detector. The elliptical mirror and the coupler were fixed on the external optical platform. With an external detector, a sample compartment was built up. The measuring system can measure fibers with lengths from several centimeters to several meters.

The coupler is one of the most important components. It has great influence on the coupling efficiency and measured attenuations. We designed and fabricated two kinds of coupler for the system. One is a silver-coated hollow waveguide coupler. The other is a silver-coated hollow tapered coupler [8]. The inner diameter at the output end is the same as the measured fiber for both couplers. This helps to achieve the stability of coupling efficiency. Figure 2 shows pictures of the two couplers and their expected focusing

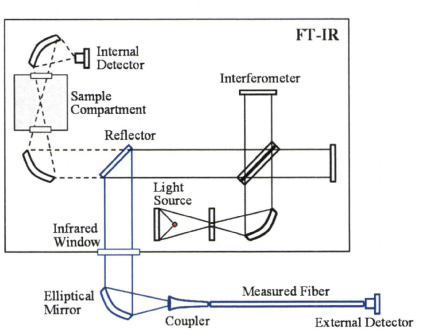

Fig. 1. (Color online) Schematic diagram of the measuring system.

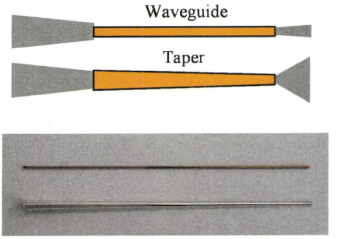

Fig. 2. (Color online) Pictures and focus images for a waveguide coupler and a tapered coupler.

properties. The tapered coupler accepts more energy because of its larger bore size at the input end. This results a good coupling efficiency. On the other hand, a tapered coupler may cause a larger divergence angle for the output light. It excites more higher-order modes with high propagation losses in the fiber.

Two kinds of hollow fiber were selected as the samples for the test measurement. They were inner coated with films of AgI/Ag [9] and OC300/Ag [10]. As shown in Fig. 3, loss spectra were measured with both couplers for the two fibers. Figure 4(a) is the loss spectra for AgI/Ag-coated hollow fiber. The length of the fiber is 1107 mm and the inner diameter is 0.7 mm. The loss peak at a 2 μm wavelength is caused by the interference of light in the thin AgI film. Peaks

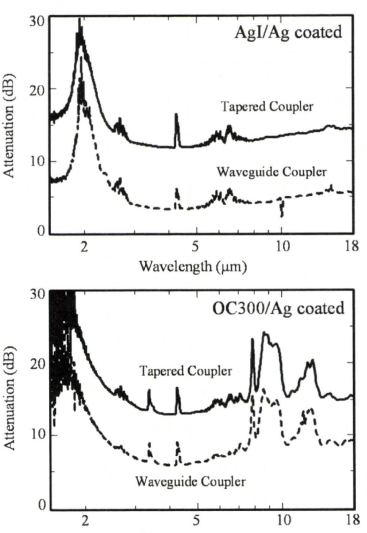

Fig. 3. Measured loss spectra of leaky infrared hollow fibers using different couplers.

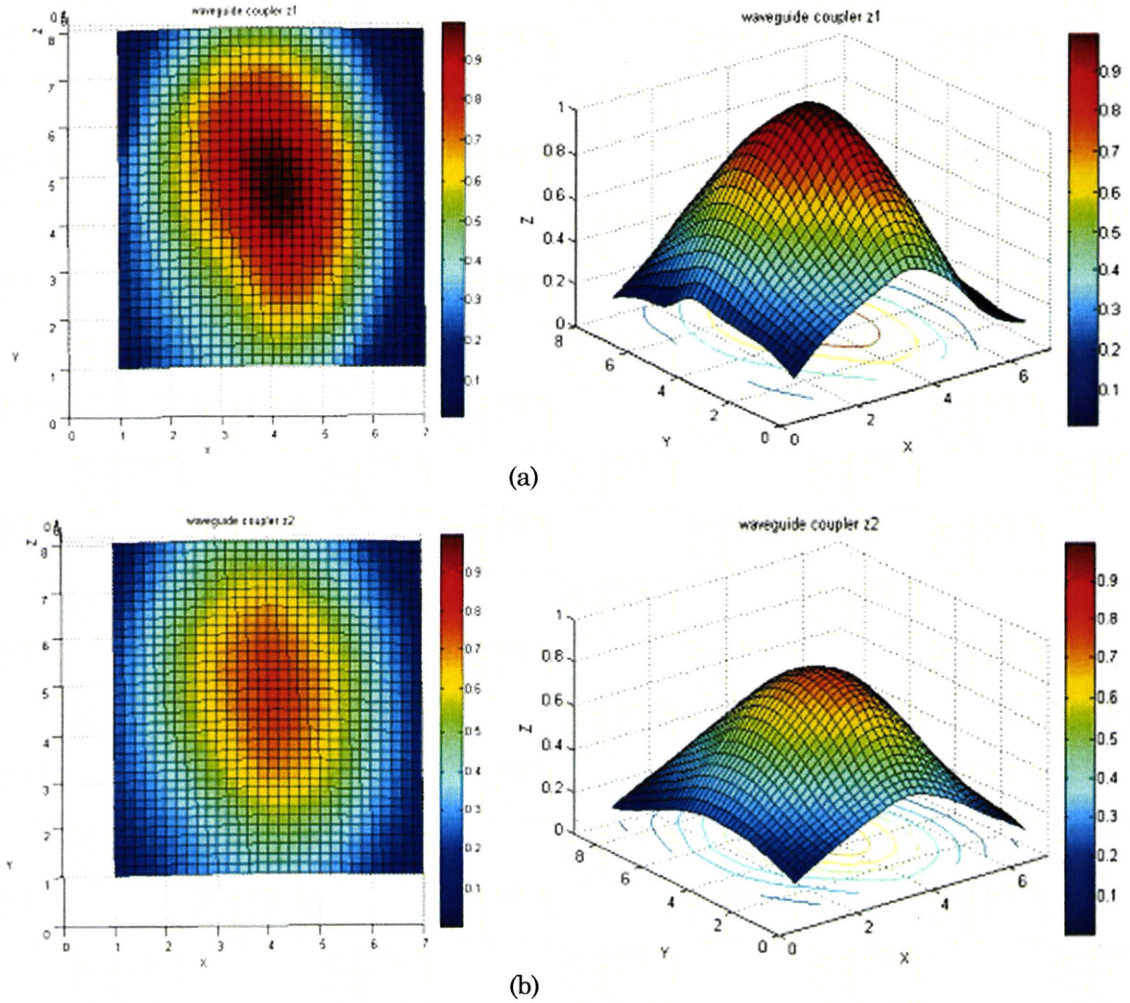

Fig. 4. (Color online) Light intensity distribution at the output end of the fiber coupler. (a) Plane Z_1 and (b) plane Z_2 were 1.5 and 3 mm from the output end, respectively.

at wavelength bands of 4.3 and 6 μm are caused by the absorption of CO_2 gas and water vapor in the air. Figure 3(b) is the loss spectra of OC300/Ag-coated hollow fiber. The length of the fiber is 785 mm and the inner diameter is 0.7 mm. Peaks at the wavelength band of 3.5 and 8–13 μm are caused by the intrinsic absorption of the OC300 film. Fibers were measured several times in a few days. A repeatable loss spectrum was obtained for both couplers. However, we note that the spectrum has different attenuation values even for an identical fiber when using different couplers.

3. Discussion

Analysis indicated that the attenuation of hollow fiber is dependent on the coupling conditions of the light source [11]. A larger divergence angle will excite more higher-order modes, which causes higher loss. We measured the divergence angles at the output ends of both couplers. Take two normal planes at the output end of the coupler and scan the light intensity. Figure 4 shows the two- and three-dimensional intensity distributions at the planes Z_1 and Z_2, which were 1.5 and 3 mm from the output end. We obtained full width at half-maximum (FWHM) of light at each plane according to the distribution. The divergence angle of the light can be calculated by using the two FWHM values and the distance between the normal planes. Measurement results showed that the divergence angle was dependent on the length of the coupler. When the waveguide-type coupler has a length of 120 mm, the divergence angle was 9.7° along the X axis and 19.5° along the Y axis. The light intensity showed an approximately Gaussian distribution. It means that most energy was in a low-order mode. The same measurements were made on the tapered coupler. The light intensity distribution is shown in Fig. 5 and the divergence angles were 16° and 98° along the X axis and the Y axis, respectively. As lots of high-order modes exist, the distribution shows several high-intensity spots. Moreover, intensity distributions for both couplers were elliptical because of the properties of the light source. The MIR light source of FT-IR is a globar, a heated silicon carbide rod.

The transmitted power $P(z)$ in hollow fibers can be expressed as [12]

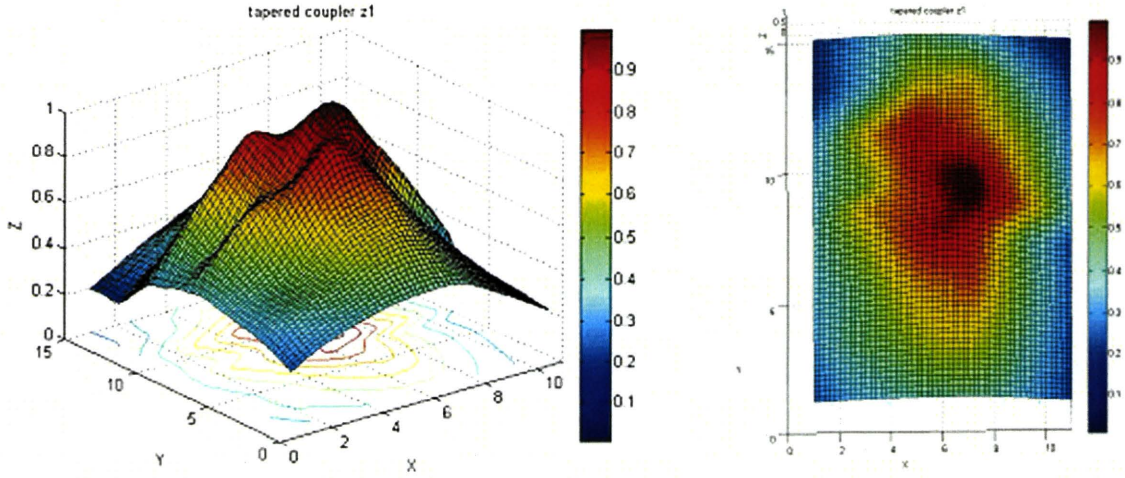

Fig. 5. (Color online) Light intensity distribution at the output end of the tapered coupler.

$$P(z) = \int_0^{\theta_{\max}} p(\theta_z) \exp\{-[1 - R(\theta_z)]z/2T \cot\theta_z\} \sin\theta_z d\theta_z, \quad (1)$$

where $\theta_{\max}$ is the maximum launching angle, $p(\theta_z)$ is the angular distribution of the launching power, $R(\theta_z)$ is the power reflection coefficient of the light, and T is the inner diameter of the fiber. By taking into consideration the divergence angle, the film thickness, and surface roughness, we obtained the calculated result for the loss spectrum.

A cyclic olefin polymer (COP)/Ag-coated hollow fiber [13] was used for the comparison of calculated and measured spectra. The fiber is 1003 mm long, with a 0.7 mm inner diameter. The calculated and measured loss spectra using different couplers are shown in Fig. 6. Peaks at the wavelengths of 2 and 4 μm are caused by the interference of light in the thin COP film. Sharp peaks at 3.5 and 7 μm are caused by the absorption of the COP. In the spectrum calculation, film thickness, film surface roughness, and the beam divergence angle were adjusted to match the measured results. Calculation results showed that the COP film thickness was 0.85 μm and the surface roughness was 30 nm in root mean square (rms). The divergence angles in the calculation were 15° and 45° for the waveguide coupler and the tapered coupler, respectively. Considering the influence of an elliptical intensity distribution of the light beam (in the calculation, the intensity was assumed to be of circular distribution), the results agree well with the measured results. The divergence angles used in the calculation were reasonable. The absorption peaks at the wavelengths of 3.5 and 7 μm disappeared in the calculated spectra because we did not take into consideration the material absorption for the polymer layer in the calculation.

We also made the calculation and measurement for two ATR-type hollow fibers, GeO_2 coated hollow glass fiber and hollow sapphire fibers. The GeO_2 fiber is 300 mm long and 1.4 mm in inner diameter. Figure 7 shows the loss spectra for measured and calculated results. Low-loss windows can be found at the wavelength bands of 7.6 and 10–12 μm. These low-loss wavelength bands are caused by the properties of the materials of the base tube (SiO_2) and inner-coated film (GeO_2). The inset in Fig. 7 shows the loss spectra for the glass-based tube. The refractive index n is less than 1 for SiO_2 around 7.6 μm. n of GeO_2 is less than 1 around 10–12 μm. Sol-gel GeO_2 coatings were deposited into silica glass substrate

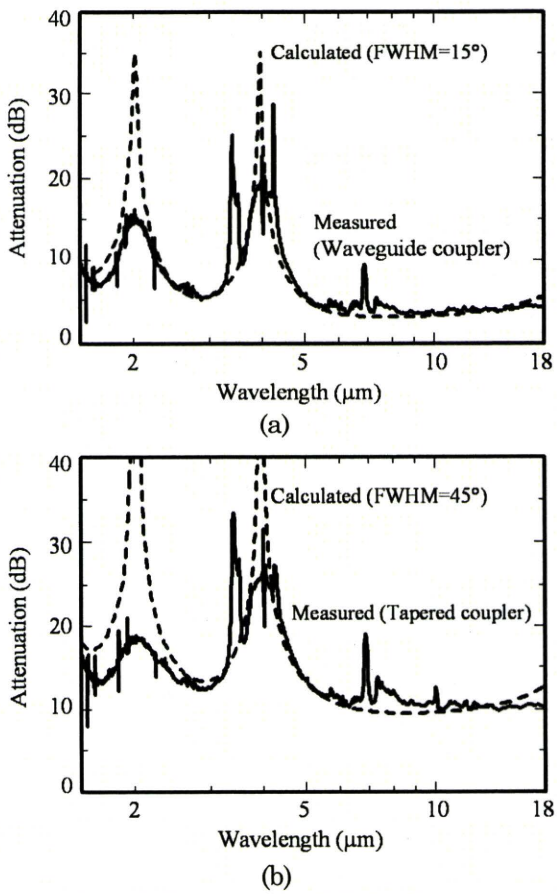

Fig. 6. Calculated and measured loss spectra using (a) the waveguide coupler and (b) the tapered coupler.

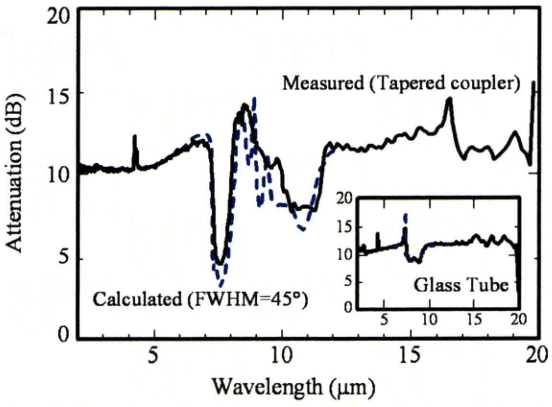

Fig. 7. (Color online) Calculated and measured loss spectra for a GeO_2 coated hollow glass fiber.

by cycles of a dip-coating operation. Since the thickness of a single layer of GeO_2 produced in this way was typically limited to less than 0.4 μm, several cycles were needed to build up uniform thick coatings. According to the fabrication parameters, the GeO_2 film was of 2.8 μm thickness in the theoretical calculation. The surface roughness was 80 nm in rms. Loss peaks in calculation results at 8.9 and 9.4 μm were caused by the multilayered film antireflection. Sharp antireflection peaks disappeared in the measured loss spectrum. This is because the accumulated thick GeO_2 film has a rather rough surface. The hollow sapphire fiber, a product of Saphikon, Inc., has a length of 990 mm and an inner diameter of 1 mm. Figure 8 shows the loss spectra. The low-loss area was found from 10 to 17 μm. This is because the refractive index n of Al_2O_3 is less than 1 in the wavelength band. In the calculation, the divergence angle is 45°.

We note that the theoretical loss spectra are in good accordance with the measured results both in low-loss wavelength bands and the absorption peaks in Figs. 7 and 8. This means that the measured spectrum from the system is reliable. Furthermore, both the ATR fibers have a low-loss property around 10.6 μm, which makes them suitable for delivering CO_2 laser light. The data of refractive indices for

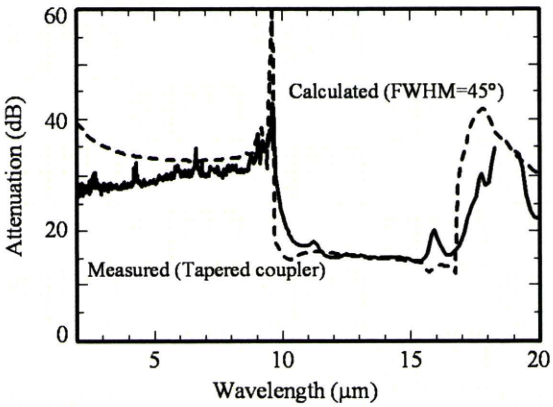

Fig. 8. Calculated and measured loss spectra for a hollow sapphire fiber.

GeO_2, SiO_2, and Al_2O_3 (sapphire) used in the calculations are taken from published literature [14,15].

4. Conclusions

Based on a commercially available FT-IR spectrometer, a beam was guided out of the FT-IR and a new sample compartment was built on the optical platform with an external detector. The loss spectra of hollow fibers with lengths ranging from several centimeters to 3 m can be measured. We designed and fabricated two couplers, a waveguide coupler and a tapered coupler, to achieve repeatable spectrum and easy coupling. The attenuation values changed when different couplers were used, even for the identical fiber, because of the influence of the divergence angle of the incident light source. The experimental and theoretical results are helpful in the improvement of the coupling methods of the infrared spectrum measuring system and the design of infrared fiber sensors.

This research is financially supported by the National Natural Science Foundation of China (NSFC) (60971014), the National Basic Research Program of China (2010CB328300), and the 211 Project for construction of key disciplines, as well as by the Health and Labor Science Research Grants (H20-nano-young-010), Japan.

References

1. M. Mohebbi, "Transmission characteristics of femtosecond optical pulses in hollow-core fibers," Opt. Commun. **253**, 290–300 (2005).
2. S. Sato, Y. W. Shi, Y. Matsuura, M. Miyagi, and H. Ashida, "Hollow waveguide based nanosecond, near-infrared pulsed laser ablation of tissue," Lasers Surg. Med. **37**, 149–154 (2005).
3. S. S. Kim, N. Menegazzo, C. Young, J. Chan, C. Carter, and B. Mizaikoff, "Mid-infrared trace gas analysis with single-pass Fourier transform infrared hollow waveguide gas sensors," Appl. Spectrosc. **63**, 331–337 (2009).
4. M. Miyagi and S. Kawakami, "Design theory of dielectric-coated circular metallic waveguides for infrared transmission," J. Lightwave Technol. **2**, 116–126 (1984).
5. C. C. Gregory, and J. A. Harrington, "Attenuation, modal, and polarization properties of $n < 1$, hollow dielectric fibers," Appl. Opt. **32**, 5302–5309 (1993).
6. C. B. Jing, J. X. Hou, and X. G. Xu, "Fabrication and optical characteristics of thick GeO_2 sol-gel coatings," Opt. Mater. **30**, 857–864 (2008).
7. R. K. Nubling and J. A. Harrington, "Optical properties of single-crystal sapphire fibers," Appl. Opt. **36**, 5934–5940 (1997).
8. Y. Matsuura, H. Hiraga, Y. Wang, Y. Kato, M. Miyagi, S. Abe, and S. Onodera, "Lensed-taper launching coupler for small-bore, infrared hollow fibers," Appl. Opt. **36**, 7818–7821 (1997).
9. R. George and J. A. Harrington, "Infrared transmissive, hollow plastic waveguides with inner Ag-AgI coatings," Appl. Opt. **44**, 6449–6455 (2005).
10. K. Iwai, M. Miyagi, Y. W. Shi, X. S. Zhu, and Y. Matsuura, "Infrared hollow fiber with a vitreous film as the dielectric inner coating layer," Opt. Lett. **32**, 3420–3422 (2007).
11. R. K. Nubling and J. A. Harrington, "Launch conditions and mode coupling in hollow-glass waveguides," Opt. Eng. **37**, 2454–2458 (1998).